THE JOURNAL OF PHYSICAL CHEMISTRY C
A JOURNAL OF THE AMERICAN CHEMICAL SOCIETY

pubs.acs.org/JPCC Article

Readout of Oriented Triplet Excitons in Linear Acenes via Room-Temperature Electrically Detected Magnetic Resonance

Taylor W. Wagner, Paul Niyonkuru, Justin C. Johnson, and Obadiah G. Reid*

Cite This: https://doi.org/10.1021/acs.jpcc.4c02941 Read Online

ACCESS | Metrics & More | Article Recommendations | Supporting Information

ABSTRACT: Optically generated molecular spin centers offer an attractive platform for room-temperature spintronic and quantum applications. The linear acene family of molecules are especially good candidates due to their efficient generation of highly polarized triplet excitons via singlet fission. However, the direct detection and manipulation of these spin centers in thin films via the electrical means desirable for ultimate microelectronic devices has proven challenging. In particular, highly oriented triplet features have previously been detected in crystalline anthracene but longer acenes reveal only doublet features in Electrically-Detected Magnetic Resonance (EDMR). In this work we present EDMR spectra of highly oriented triplet excitons in pentacene for the first time, using a host−guest style device made of tetracene and pentacene. The guest acts as an energetic trap site, permitting the isolation and detection of molecular triplets at room temperature. Modeling of these results shows that the observed resonance features correspond to triplet sublevel transitions on isolated pentacene guest molecules. Rotation of the applied field confirms the tendency of the linear acenes to self-orient with the longest molecular axis perpendicular to the device substrate. Lastly, we find the disappearance of resonant triplet features in the neat acenes is not primarily due to the effects of exciton delocalization, but a broader mechanism of spin relaxation primarily influenced by exciton diffusivity.

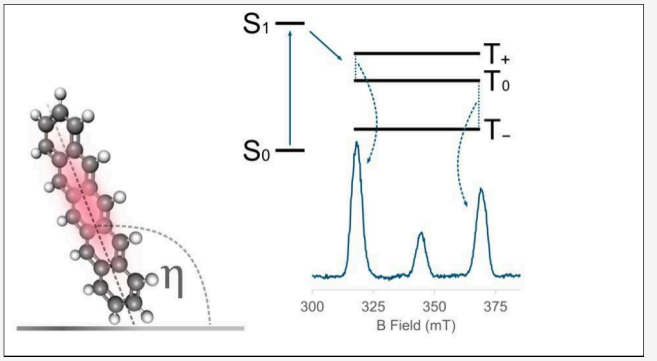

INTRODUCTION

Molecular semiconductors are promising candidates for many modern electronic technologies like spintronics, novel photovoltaics, quantum computing, and quantum sensing.[1,2] The ease of synthesis, low cost, and tailorability of these materials makes them generally appealing, and their inherent low spin−orbit coupling is highly attractive for applications that require long-lived room temperature spin centers or efficient spin transport.[3] Recent advances in molecular coherence times and gate operation speeds utilize the coupling between excited electronic states and nearby magnetic nuclei, and promise the ability for individual molecules to act as hybrid qubit systems.[4−6] Electronic states excel at pure state preparation at room temperature due to strong coupling to electromagnetic fields, while substituent magnetic nuclei boast sufficiently long spin coherence times to act as quantum memory.[7] These impressive systems motivate the need for electrical readout, as optical schemes require bulky setups that prevent the realization of miniature devices that will ultimately be desired either for sensing or computing applications.[8] Similar to quantum dot systems that incorporate the Pauli blockade principle, a single molecular photoexcited state could in principle prevent or facilitate charge transfer based solely on spin polarization.[9−11] Such a system would offer a straightforward pathway to the realization of practical electrical readout with single molecule sensitivity at reasonable temperatures.

This approach can find utility in the near-term in quantum sensing applications where molecular ensembles are appropriate, and in the long run there is potential for computing if the limit of single-molecule measurements is reached.[12,13] For practical sensing, all that is required is a method of hyperpolarizing a spin system, and a simple sensitive method, like electric current, for reading out its coherence time, as this provides extremely sensitive measurements of the local magnetic environment.[14] Computing applications are much more challenging, requiring an electrical interface with a single molecule,[12,13] and ultimately remote entanglement of multiple molecular spin centers.[15]

Toward this goal, we propose a system where the long-lived triplet exciton serves the role of the excited electronic state, facilitating readout and initialization, and the phenomenon of

Received: May 4, 2024
Revised: June 21, 2024
Accepted: June 24, 2024

Singlet Fission (SF) serves as the initialization mechanism.[7,16−22] The purpose of this paper is to discover how and if electrical readout of the triplet excitons is possible in such systems. We focus here on the linear acene family of molecules, because they are sufficiently conductive to support large current densities, and excel at generating well-ordered room temperature triplet species from SF.[23−27]

Singlet Fission, as shown in Figure 1, is a process in which an initial excitation in the first excited singlet state partitions its energy into two neighboring first excited triplet states.[33−35] The kinetics of SF can be modified based on the first excited state energies of the acene involved, and the resulting triplet spins can even be purposefully localized via chemical synthesis, for example in bridged dimer configurations[16,27,36−38] that confer control over the initially generated spin population via their orientation within an applied magnetic field.[16,38,39] The process is also spin-conserving, producing two spin-polarized triplet pairs that could then be manipulated and read out in an ensemble electrically detected measurement scheme we test here.[35,40,41]

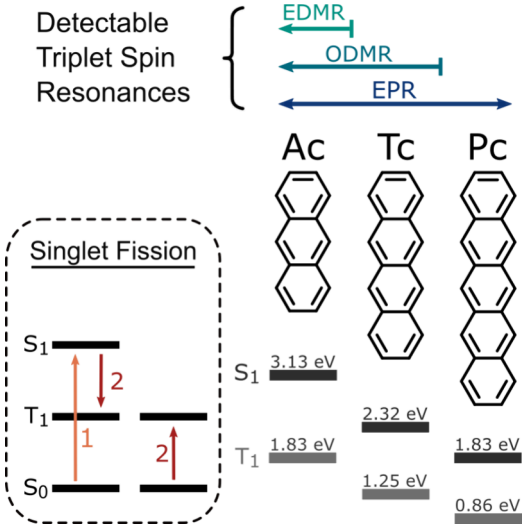

Figure 1. Bottom left: Singlet fission process, whereby one chromophore is excited into the first excited singlet state and proceeds to fission to a neighboring molecule to produce two first excited triplets. Right: Single crystal excited-state energies for anthracene (Ac),[28,29] tetracene (Tc),[30] and pentacene (Pc)[31,32] and which molecules display triplet features based on magnetic resonance scheme.

Electrical readout of triplet states in linear acenes might be achieved via a magnetoconductance (MC) measurement, whereby photoexcited triplet states are probed through their interaction with mobile charges.[42−44] The triplet-charge interaction is only one of many mechanisms that explains Organic Magnetoresistance (OMAR) commonly observed in organic semiconductors, but forms the basis for the present measurement scheme.[45−49] As seen in Figure 2, mobile charges approaching an occupied trap site can either pass by or undergo a triplet-charge interaction with two outcomes. Based on the total spin of the complex, a spin-allowed (doublet character) configuration results in quenching to the molecular ground state, whereas a spin-forbidden configuration (quartet character) eventually sees the two constituent particles scatter apart. The triplet-charge complex forms a set of mixed quantum states, and the ratio of scattering to quenching

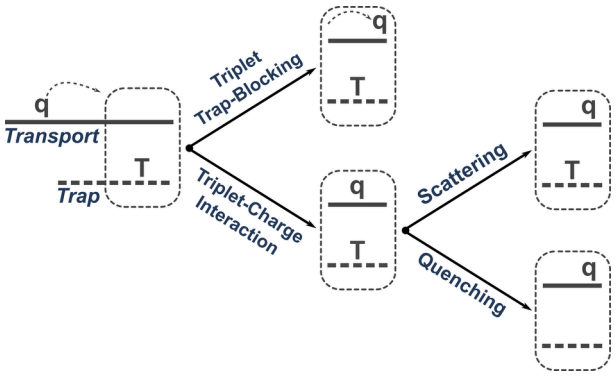

Figure 2. A mobile charge q can avoid interaction through a triplet T trap-blocking mechanism or undergo a triplet-charge interaction. The total spin of the triplet-charge complex is field-dependent and determines if the complex eventually scatters apart or the triplet is quenched to the ground state.

events becomes magnetic field-dependent, as the probability of forming doublet configuration complexes decreases at high magnetic field.[43] This in turn leads to a field (and spin) dependence of the conductance, as the change in quenching probability modulates the ratio of trapping to scattering events.[50] While intrinsic trap sites are not required for the interaction to occur, modeling of the triplet-charge interaction has revealed that both trap density and triplet-trapping can profoundly amplify the resulting MC.[50,51]

Because of the apparent benefit of energetic trap sites in studying the triplet-charge interaction, we investigate a host−guest system in this work, where the guest material acts as an intentionally engineered trap site to isolate and probe molecular triplets. We chose pentacene (Pc) as the guest and tetracene (Tc) as the host molecule due to their identical crystal packing and energetic alignment. Pc is an optimal choice as guest material, as it is very well studied, boasts sufficient conductivity, and exhibits a notably low ionization potential and triplet state energy.[52] Tetracene as a host material facilitates triplet generation through SF, and its excitonic state energies and ionization potential promote both exciton and charge transfer to the guest Pc molecule. It also possesses a crystal structure identical to that of Pc, making clean substitutional doping of Tc crystals with Pc guests possible.[53−55] In this host−guest architecture, the Tc host is directly optically excited to induce SF, while the Pc acts as a triplet acceptor and trap site. The singlet-fission dynamics of Tc/Pc blends have been studied, and it was observed that both acenes undergo homofission with a small contribution from heterofission between each species.[31,56,57] It was reported that even at low Pc guest concentrations, the triplet exciton population was dominated by those localized on Pc on a time scale of 10−100 ps.[55]

Detection of triplet spins can be accomplished by driving triplet sublevel transitions with microwaves through a variety of magnetic resonance techniques. There are however unanswered questions that have arisen from the different experimental spectra obtained for the linear acenes based on detection scheme. As seen at the top of Figure 1, not all magnetic resonance techniques have been able to observe triplet sublevel transitions within the series. Anthracene is well-studied and displays strong triplet and doublet features via Electrically Detected Magnetic Resonance (EDMR), but similar studies of Tc and Pc reveal only doublet

https://doi.org/10.1021/acs.jpcc.4c02941
J. Phys. Chem. C XXXX, XXX, XXX−XXX

features.[54,58−63] The Optically Detected Magnetic Resonance (ODMR) scheme measures the change in optical emission or absorption of a specific state under resonant conditions, and has been used to observe oriented triplet features in Tc.[64,65] Electron Paramagnetic Resonance Spectroscopy (EPR) typically involves modulation of the applied field and measures the resulting change in reflected microwave intensity.[24,66] EPR experiments are often conducted with dilute solid state samples under cryogenic conditions to limit spin−lattice relaxation effects, and have successfully revealed triplet features in all three acenes.[18,19,52,67]

In this work, we investigate the electrical readout mechanism of triplet spin states described above using both pure and host−guest systems of linear acenes and resolve the reported differences in magnetic resonance detection schemes.[50] We find that the exciton-charge interaction can indeed be used to detect the exciton spin state electrically, and present EDMR spectra that evince highly oriented triplet features of guest Pc in host Tc. The orientation-dependence of the sublevel transitions we observe is consistent with triplet spin transitions on isolated pentacene molecules with their tertiary magnetic axis (X) oriented 11.9° from the surface normal. Varying the guest loading shows that the triplet EDMR features disappear as the concentration increases, consistent with the falling probability that guest molecules randomly distributed in a host matrix are completely isolated from each other. These results provide a coherent explanation for the counterintuitive absence of triplet features observed in previous EDMR experiments on pure Tc and Pc: spin−lattice relaxation caused by hopping events destroys the spin polarization needed to observe them.

METHODS

All measurements reported in this work were performed at room temperature using devices fabricated on 10 × 30 mm^2 glass/ITO substrates, either held within a rectangular waveguide microwave resonator or mounted on a coplanar waveguide loop antenna for cryogenic measurements. The ITO on glass substrates were etched as previously described.[50] Device layers were deposited in a bottom-up fashion starting with a thin hole transport layer of spin-coated PEDOT:PSS, followed by a thermally evaporated polycrystalline acene layer, followed by a Gold−Silver top electrode. Al 4083 Ossila PEDOT:PSS, 99.9% sublimed grade pentacene, and 99.99% sublimed grade benz[b]anthracene (tetracene) were used as supplied. Both PEDOT:PSS and gold were chosen to promote hole injection and extraction for the primarily hole-only device architecture.[68−71]

MC measurements were performed via electrical modulation of the input current and subsequent detection of the lockin R-channel as a function of applied field. EDMR measurements were taken in a similar fashion, where the RF microwave signal was instead modulated and the resulting current change was amplified and detected in both in-phase and out-of-phase channels. A Pyramid Hall Probe was used to determine the real magnetic field strength with ±0.6 mT accuracy. Samples were rotated with respect to the applied field by rotation of the whole microwave cavity and waveguide apparatus to ±1° accuracy. All EDMR curves reported in this work were measured for a minimum of 4 h and repeated with several devices to ensure reproducibility.

RESULTS AND DISCUSSION

Acene-based devices were fabricated to enforce hole-only transport as a way to suppress other commonly seen organic magnetoresistance mechanisms, namely bipolaron formation and electron−hole pair interconversion. The hole transport layer of PEDOT:PSS and direct gold electrode contact provide an alignment of the molecular conduction bands and metallic Fermi level such that electron transport is discouraged by a high injection barrier.[50] As seen in Figure 3, all three types of

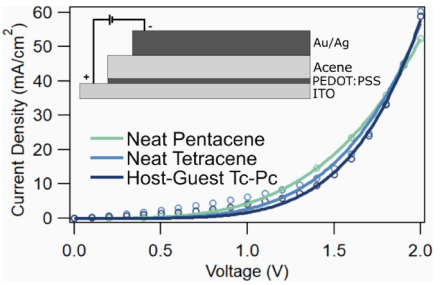

Figure 3. Current−voltage characteristics of neat acene devices and a (99%Tc/1%Pc) host−guest device. Inset: Device stack.

acene layers exhibit very similar current densities around the standard 1 V operating conditions. Pentacene was introduced as a guest between 0.1 and 20% loading via simultaneous codeposition. In this scheme, pentacene acts as a mobile charge and exciton trap site because of its lower ionization potential and first excited state energies compared to the host tetracene.

Trap density and the effectiveness of trapping has been shown to be critical in the observance of triplet-charge magnetoresistance effects.[50,51] We analyze the current−voltage relationship of all three devices using the Mark-Helfrich equation, which is derived under the assumption of ideal space-charge limited conduction influenced by characteristic trap sites:[72]

$$J = q^{1-l}\mu_n N_c \left\{ \frac{\epsilon_0 \epsilon_r l}{N_t (l+1)} \right\}^l \left\{ \frac{2l+1}{l+1} \right\}^{l+1} \frac{V^{l+1}}{L^{2l+1}} \quad (1)$$

Here, J is the current density, q is the elementary charge, μ_n is the carrier mobility, N_c is the effective density of states at the relevant transport band, ϵ_0 and ϵ_r are the vacuum and relative permittivity respectively, N_t is the effective trap density, V is the bias voltage, and L is the length of the active layer. l is a representation of the trapping frequency, with higher values representing either deeper trap sites and/or more effective molecular trapping mechanisms. From the fitting, l was found to be lowest with neat Pc (2.58), moderate with neat Tc (3.49), and highest with the host−guest system (4.08). While the fitting does not provide explicit details on the trapping mechanism, it does imply the conduction pathways for the codeposited layer are more energetically disordered compared to either neat material.

The magnetoresistance mechanisms and underlying theory for neat Pc devices were thoroughly explored in our previous work.[50] We developed a quantum kinetic model based on the Hamiltonian of the weakly coupled triplet-charge interaction that explained the observed effects via a triplet-trap filling model. This explains the little to no observed MC of neat Pc devices in the dark, but the consistent large positive MC under

https://doi.org/10.1021/acs.jpcc.4c02941
J. Phys. Chem. C XXXX, XXX, XXX−XXX

illumination and subsequent triplet generation via SF. Not all photoresponsive SF materials exhibit this same effect though, as the thermodynamics of the phenomenon are field dependent.

Figure 4 shows typical MC measurements gathered by sweeping the applied field and measuring the resulting change in conductance under illumination. The magnetoconductance is defined by

$$MC = \frac{I(B) - I(0)}{I(0)} \times 100\% \quad (2)$$

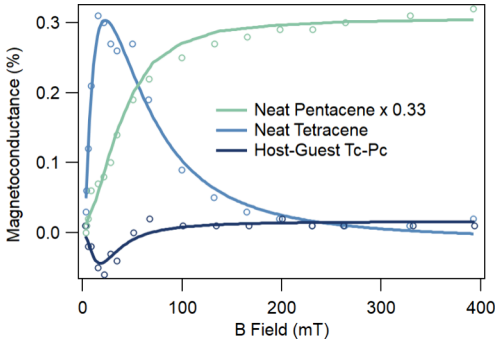

Figure 4. Magnetoconductance of photoexcited acene devices. Pc illuminated with 660 nm red light and Tc and (99%Tc/1%Pc) host−guest device illuminated with 505 nm green light. Solid lines represent fits to separate kinetic models based on the highest-concentration acene present. Pc data scaled down to one-third to increase visibility.

As seen in Figure 4, the strong positive MC effect commonly seen in Pc is not matched by the other device types. Here, Pc is illuminated with 660 nm red light, while the primarily Tc devices are illuminated with 505 nm green light. This most strongly aligns the absorption of the materials with their respective band gaps to produce similar exciton densities, as shown in the Supporting Information via absorption spectroscopy and photocurrent measurements. A key difference between the acenes is that the SF efficiency in neat Pc remains relatively unchanged during the field sweep, whereas the SF efficiency of Tc is reduced at high field. The initial increase in conductivity in neat Tc is attributed to the triplet trap-filling mechanism, whereby triplet spins generated via SF fill unoccupied lower energy states in the conduction band, blocking the site for mobile charges and increasing the effective mobility. At high field, Tc exhibits a well characterized reduction in the SF efficiency, causing the overall triplet density to fall.[23,53] As such, the MC characteristics of Tc follow a dual Lorentzian behavior, and the best fit to the experimental curve in Figure 4 reveals a low-field positive Lorentzian centered around 8 mT, and a high-field negative Lorentzian centered around 80 mT.

Interestingly, the host−guest system behaves unlike either neat film, instead displaying a primarily negative MC. It is not uncommon in OMAR studies to observe systems that retain the same fundamental curve shape, but flip sign in response to a change in bias voltage, film thickness, temperature, or even choice of electrode.[73−77] The host−guest system displays a similar dual Lorentzian behavior to that of the neat Tc film, implying a retention of the change in SF efficiency as a function of applied field. The sign change and overall reduction in magnitude could indicate a saturation of the trap-filling effect, implying that at low field the triplet density that is able to affect mobile charges is already maximized, and any additional change has little to no effect on conduction pathways. The slight positive high field MC is not statistically significant, but if this were a real effect, could suggest that the guest Pc is still providing some improvement in conduction through the triplet-charge mechanism, even in low concentration.

Figure 5 shows field-swept room temperature EDMR measurements taken on the acene devices with the current vector parallel to the static magnetic field vector. In these experiments, the device is put under the same conditions as the MC measurements, where illumination drives the generation of triplet spins through SF and a constant DC bias promotes triplet-charge interactions. An amplitude-modulated microwave-magnetic field is then applied perpendicular to the static magnetic field in order to drive spin transitions when the Zeeman splitting of a given transition matches the fixed microwave drive frequency (9.625 GHz at 20 dbm power). The conductance is then constantly measured via lockin detection at the microwave modulation frequency (1.243 kHz), and the field is swept back and forth to detect spin transitions that alter the baseline conductance.

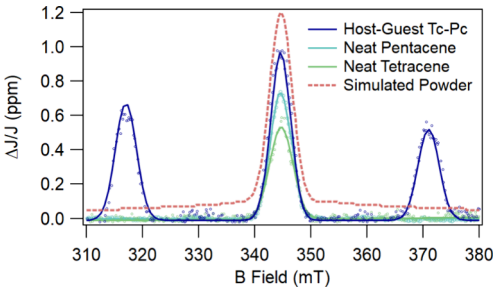

Figure 5. In-plane EDMR spectra of neat acene devices and a (95% Tc/5%Pc) host−guest device at a carrier frequency of 9.625 GHz. Also shown is the simulated powder spectrum from the subsequent analysis revealing one heavily broadened feature.

From Figure 5, all three devices exhibit a clear center-field spectral feature, which can be attributed to the symmetric doublet electron transition. But only the host−guest device exhibits wing features (displaced from center-field) that are attributed to oriented triplet sublevel spin transitions. The distinct orientation is evident when compared to the simulated powder spectrum, whereby the triplet contributions from different molecular orientations result in a significantly broadened centralized component. The fact that the neat acene spectra reveal no triplet features while undergoing strong SF is counterintuitive, but this is consistent with previous studies.[52,54,60,61,63] The neat acene films measured through EDMR produce only one center-field peak that fits well to a sum of Gaussian and Lorentzian line shapes, shown in the cryogenic EDMR section of the Supporting Information This center-field peak is commonly attributed not to the high triplet density from the SF process, but to mobile and trapped charges that undergo a symmetric spin flip, placing them directly at the center-field of the chosen resonant frequency. Here the 9.625 GHz frequency corresponds to a g = 2 center-field line of 344.1 mT.

The wing features seen in the host−guest device in Figure 5 are the first evidence of triplet spin transitions in Pc detected through EDMR. The peak positions correspond to specifically oriented molecular Pc triplets with respect to the applied field

https://doi.org/10.1021/acs.jpcc.4c02941
J. Phys. Chem. C XXXX, XXX, XXX−XXX

orientation. These features have already been observed electrically in anthracene and optically in tetracene, and also agree with previous literature on the preferred growth orientation of acene crystals in thermally evaporated thin films.[18,53,54,58,59,78] In order to elaborate on why these features only appear in a codeposited film and to conclusively define the molecular orientation bias in the film, we detail a theory based on the underlying Hamiltonian of the doublet-triplet system. The total spin Hamiltonian governing the triplet-charge system is given by

$$H = H_{Z,T} + H_{Z,D} + H_{hf,T} + H_{hf,D} + H_{\mathrm{zfs},T} + H_{ex}$$

$$H_{Z,i} = \frac{g\mu_B}{\hbar} B_{\mathrm{app}} \cdot S_i$$

$$H_{hf,i} = \frac{g\mu_B}{\hbar} B_{hf,i} \cdot S_i$$

$$H_{\mathrm{zfs},T} = \frac{D_{\mathrm{zfs}}}{\hbar^2} S_{T,z}{}^2 + \frac{E_{\mathrm{zfs}}}{\hbar^2}(S_{T,x}{}^2 - S_{T,y}{}^2)$$

$$H_{ex} = \sum_i \sum_j J_{ij} S_{Di} S_{Tj} \tag{3}$$

where $H_{Z,i}$, $H_{hf,i}$, $H_{zfs,T}$, and H_{ex} represent the contributions from the Zeeman splitting, hyperfine interactions, zero field splitting of the triplet state, and doublet-triplet exchange coupling, respectively. D_{zfs} and E_{zfs} are experimentally determined parameters, and the tensor J_{ij} represents the total isotropic, symmetric, and antisymmetric exchange interaction between the doublet and triplet.[79]

The Zeeman and Hyperfine terms of the Hamiltonian are initially represented in what are termed the high field basis states, having an explicit representation in terms of positive and negative contributions with respect to the applied field. The zero field splitting term in the Hamiltonian is initially represented in what is termed the zero field basis states, having an explicit representation with respect to the primary X, Y, and Z molecular axes. The zero field splitting term is first transformed and represented in the high field basis states and combined with the Zeeman and Hyperfine terms to produce six uncoupled states made up of the combinations of the triplets (T_+, T_0, T_-) and doublets (α, β). First, the zero field splitting component is given by

$$\boldsymbol{H}_{\mathrm{ZF}} = \begin{pmatrix} g\mu_b B_Z + \frac{D_{\mathrm{zfs}}}{3} & \frac{1}{\sqrt{2}} g\mu_b (B_X + iB_Y) & \frac{1}{2}(D_X - D_Y) \\ \frac{1}{\sqrt{2}} g\mu_b (B_X - iB_Y) & D_X + D_Y & \frac{1}{\sqrt{2}} g\mu_b (B_X + iB_Y) \\ \frac{1}{2}(D_X - D_Y) & \frac{1}{\sqrt{2}} g\mu_b (B_X - iB_Y) & -g\mu_b B_Z + \frac{D_{\mathrm{zfs}}}{3} \end{pmatrix} \tag{4}$$

where g is the electron g-factor, μ_B is the Bohr magneton, and

$$B_X = B_{\mathrm{app}} \sin\theta_M \cos\phi_M \tag{5}$$

$$B_Y = B_{\mathrm{app}} \sin\theta_M \sin\phi_M \tag{6}$$

$$B_Z = B_{\mathrm{app}} \cos\theta_M \tag{7}$$

$$D_X = \frac{-D_{\mathrm{zfs}}}{3} - E_{\mathrm{zfs}} \tag{8}$$

$$D_Y = \frac{-D_{\mathrm{zfs}}}{3} + E_{\mathrm{zfs}} \tag{9}$$

where B_{app} represents the strength of the applied magnetic field, and θ_M and ϕ_M represent the orientation of this applied field with respect to the conventional polar and azimuthal angles in the molecular frame. Next, the zero field basis states in the molecular frame can be transformed to compatible high field basis states by applying the high field unitary transformation matrix

$$\boldsymbol{H}_{\mathrm{HF}} = \boldsymbol{U}_{\boldsymbol{T}}^{\boldsymbol{H}} \boldsymbol{H}_{\mathrm{ZF}} \boldsymbol{U}_{\boldsymbol{T}} \tag{10}$$

where

$$\boldsymbol{U}_{\boldsymbol{T}} = \begin{pmatrix} -\cos\theta_M \cos\phi_M + i\sin\phi_M & \cos\phi_M - i\cos\theta_M \sin\phi_M & \sin\theta_M \\ \sqrt{2}\cos\phi_M \sin\theta_M & i\sqrt{2}\sin\theta_M \sin\phi_M & \sqrt{2}\cos\theta_M \\ \cos\theta_M \cos\phi_M + i\sin\phi_M & \cos\phi_M + i\cos\theta_M \sin\phi_M & -\sin\theta_M \end{pmatrix} \tag{11}$$

where rows represent $|+1\rangle$, $|0\rangle$, $|-1\rangle$ high field states and columns represent $|X\rangle$, $|Y\rangle$, $|Z\rangle$ zero field states. Lastly, the six state doublet triplet Hamiltonian is formed via the tensor product

$$\boldsymbol{H}_{\mathrm{TD}} = \boldsymbol{H}_{\mathrm{HF}} \otimes \boldsymbol{H}_D = \begin{pmatrix} H_{11} & H_{12} & H_{13} \\ H_{21} & H_{22} & H_{23} \\ H_{31} & H_{32} & H_{33} \end{pmatrix} \otimes \begin{pmatrix} \frac{1}{2} g\mu_b B_{\mathrm{app}} & 0 \\ 0 & -\frac{1}{2} g\mu_b B_{\mathrm{app}} \end{pmatrix} \tag{12}$$

The hyperfine interaction is included in relevant inner product matrix positions and averaged over many random directions. The effect is quite small and results in a negligible contribution at high field in resonance experiments but is detailed in the Supporting Information. The final exchange coupling term in the Hamiltonian is represented with an explicit form in eq 3, but it is more intuitive to view the interaction as a change from uncoupled basis to a coupled one. Instead of representing the coupling term in the molecular or Zeeman frame, we follow the common approach of formulating the Hamiltonian first in the uncoupled basis and then rotating the eigenbasis to the coupled mixed states based on the strength of the exchange and dipolar coupling.[80] In this scheme, we can define a direct relation between the uncoupled basis states on the left, the weakly coupled Ψ basis states in the middle, and the strongly coupled doublet/quartet states on the right:

$$\begin{aligned} T_{+\alpha} &= \Psi_1 = |Q_{+3/2}\rangle \\ T_{+\beta} &\approx \Psi_2 = -\sin\theta_{DT}|Q_{+1/2}\rangle + \cos\theta_{DT}|D_{+1/2}\rangle \approx |D_{+1/2}\rangle \\ T_{0\alpha} &\approx \Psi_3 = \cos\theta_{DT}|Q_{+1/2}\rangle + \sin\theta_{DT}|D_{+1/2}\rangle \approx |Q_{+1/2}\rangle \\ T_{0\beta} &\approx \Psi_4 = \cos\phi_{DT}|Q_{-1/2}\rangle + \sin\phi_{DT}|D_{-1/2}\rangle \approx |Q_{-1/2}\rangle \\ T_{-\alpha} &\approx \Psi_5 = -\sin\phi_{DT}|Q_{-1/2}\rangle + \cos\phi_{DT}|D_{-1/2}\rangle \approx |D_{-1/2}\rangle \\ T_{-\beta} &= \Psi_6 = |Q_{-3/2}\rangle \end{aligned} \tag{13}$$

In these basis representations, a lack of exchange coupling would result in retention of the high field states on the left and infinitely strong coupling would produce the fully coupled doublet-quartet basis states on the right. The canonical eigenbasis rotation angles θ_{DT} and ϕ_{DT} represent the strength

https://doi.org/10.1021/acs.jpcc.4c02941
J. Phys. Chem. C XXXX, XXX, XXX−XXX

of the coupling, and thus the extent of the rotation of the eigenbasis. In studies of the magnetoresistance of the neat linear acenes, the weakly coupled Ψ or strongly coupled doublet-quartet states are invoked to explain the root cause of the magnetic field effects.[43,46,50,51]

It is clear from these studies that thin films of neat acenes provide an environment that fosters triplet-charge interactions. But it is not apparent whether the triplet and charge are required to be weakly or strongly coupled in this scheme, or perhaps fleeting interactions with no exchange coupling dominate the mechanism. In particular, in the following EDMR results we find little to no evidence of doublet-triplet exchange coupling in the host−guest matrix, but instead isolated doublets and triplets. In the following modeling we choose the Ψ basis convention to describe the 6 doublet-triplet states, but with no exchange coupling these are synonymous with the high field (T_+, T_0, T_-) and (α, β) states. Explicit forms of the coupled basis states, eigenenergies, and exchange coupled EDMR simulation are provided in the Supporting Information

In order to simulate the EDMR, special care must be taken to clarify the molecular orientation with respect to the applied field. Figure 6a depicts the fixed magnet pole in the lab frame

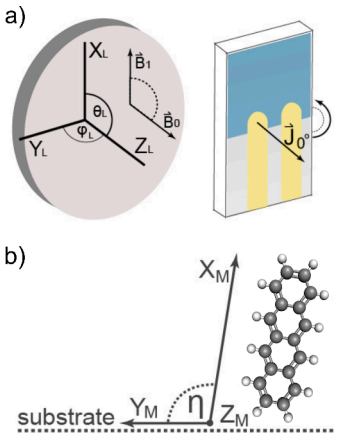

Figure 6. Relevant experimental orientations. a) Laboratory frame consisting of a magnetic pole and device, where the static field B_0 is fixed parallel to Z_L. Physical rotation of the device in the X_LZ_L plane rotates the current vector and the microwave-magnetic field B_1. b) Molecular frame of tetracene, highlighting the tendency of evaporated films to align with respect to the substrate surface.

with the static field B_0 always pointing in the Z_L direction. A device substrate is allowed to rotate within the applied field along the angle θ_L in the X_LZ_L plane. Devices are fabricated in such a way where the active area is defined by the overlap between the underlying ITO (blue) and vertical metal finger electrode (yellow). The initial configuration when θ_L is equal to 0 requires the current vector J and static field B_0 to point along Z_L, while the microwave-magnetic field B_1 points perpendicular along the X_L direction. When the device is rotated a full 90°, the current vector now points along the X_L direction and both the static and microwave-magnetic field B_0 and B_1 point along the Z_L direction.

The molecular frames for both acenes are defined based on the conventional X_M, Y_M, and Z_M molecular axes.[18] Figure 6b shows the orientation of these axes with Tc as an example, and highlights the propensity of acene molecules to align themselves standing up on the device substrate, as is typical in thermally deposited films.[53,55] Both Pc and Tc tend to align with the X_M-axis mostly normal to the plane of the substrate in a herringbone fashion.[18] The orientations in the Y_M and Z_M directions tend to be isotropically distributed, and it is believed this stacking motif maximizes the beneficial pi-pi stacking along the X_M-axis of the acenes.[78] Due to the similarities in structural conformation and crystal dimensions, Tc and Pc blends from thermal codeposition form solid solutions, and lattice sites are presumed to be occupied randomly.[55] The tilt angle of the acenes standing on the substrate surface is represented here as η, but is really a more complex combination of angles α and β of the unit cell parameters. We will approximate the EDMR simulations using this singular tilt angle η, but the full unit cell parameters for both acenes are included in the Supporting Information

Figure 7 depicts the Pc EDMR simulation procedure from initial construction of the full doublet-triplet Hamiltonian to the resulting EDMR plot as a function of molecular orientation. In Figure 7a, the energy levels of the separated doublet and triplet species and the six combined Ψ states are graphically represented. The spin up α to spin down β

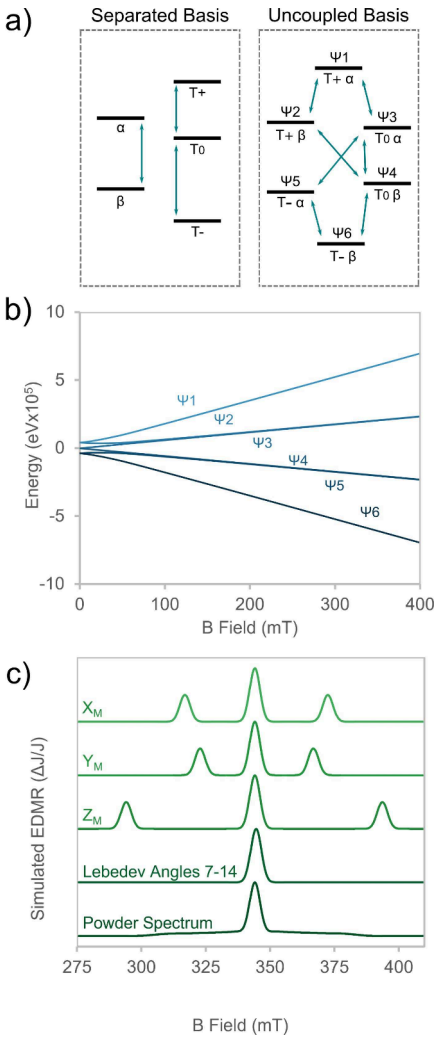

Figure 7. Theoretical EDMR simulation. a) Basis states of the doublet and triplet species and possible transitions. b) Zeeman splitting of the resulting six state Hamiltonian of Pc. c) Simulated Pc EDMR based on orientation of the applied field with respect to the molecular axes.

https://doi.org/10.1021/acs.jpcc.4c02941
J. Phys. Chem. C XXXX, XXX, XXX−XXX

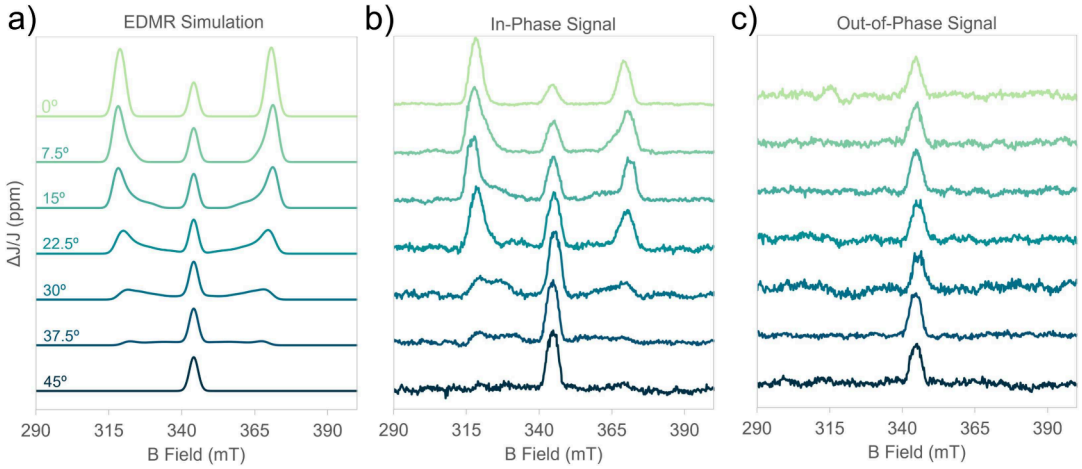

Figure 8. Waterfall plots of a) simulated and b) experimental in-phase and c) out-of-phase EDMR of a (99%Tc/1%Pc) host−guest device with respect to device rotation angle θ_L within the X_LZ_L plane of the laboratory frame. The data shown was rephased in post to minimize signal amplitude in the out-of-phase channel.

transition is symmetric while the two triplet transitions are asymmetric due to the zero field splitting of the acene. In the uncoupled basis states, there are now 7 possible state transitions, 3 represent a pure doublet spin flip, and 4 represent a pure triplet sublevel transition. With no exchange coupling, the transitions are degenerate, still producing only 3 unique resonances, and the system is still treated effectively as pairs of isolated spins. Figure 7b shows the state energies resulting from the doublet-triplet Hamiltonian as a function of applied field. This depiction changes slightly based on the choice of molecular orientation with respect to the applied field. When the applied field is oriented parallel to the shortest Z_M-axis of the molecule, the asymmetry becomes the most pronounced, and the eigenenergies of the T_+ to T_0 transition and T_- to T_0 transition are separated by the largest possible splitting.

The simulated spectra in Figure 7c are produced by first calculating the Ψ state energies assuming a fixed microwave resonance of 9.625 GHz. The splitting of the state energies is converted into corresponding applied field units via the following relation

$$\Delta E_{ij} = h\omega_{ij} = g\mu_b B_{ij} \tag{14}$$

where Planck's constant h is used to convert the difference in energies between Ψ states i and j into a transition frequency. The applied field strength that corresponds to the 9.625 GHz transition is found and a Gaussian broadening is applied to each transition line in Figure 7c. The width of the Gaussian broadening is chosen to most closely match experimental data, and is attributed to the combination of hyperfine interactions of nearby hydrogen nuclei and the precision of the experimental apparatus.

EDMR simulations are shown in Figure 7c for four different molecular orientations with respect to the applied field, and an isotropic powder. When the principle magnetic axes of the molecule are aligned with the applied field, a single peak due to the doublet transitions appears at center-field, while two distinct wing peaks appear to the left and right of center-field due to the triplet transitions. The zero field splitting parameters determine the separation of the wing peaks, with the shortest primary Z_M-axis displaying the largest splitting of $2D_{zfs}$ between the triplet peaks. To simulate the nonprimary crystal axes, we generate a series of angles based on the Lebedev quadratures, which to a certain degree of accuracy are able to simulate an averaging of spherical systems without biasing the primary axis directions.[81] Lebedev angles 7−14 at precision 5 all produce the same simulated EDMR spectrum, as the triplet eigenenergies are no longer steeply split by any of the primary crystal axes. This results in the triplet and doublet transitions all contributing to one large central peak. The simulated powder spectrum was generated via averaging over 10,000 random angles, and produces a heavily pronounced center-field feature due to the doublet transitions and many of the triplet transitions. From these predictive spectra, it is clear that the wing peaks observed in the host−guest EDMR in Figure 5 must be due to triplets on molecules oriented with one of their principal magnetic axes parallel to the applied field.

The triplet wing features observed in the host−guest device in Figure 5 align quite well with the simulated spectrum of doublet and triplet transitions of Pc oriented with their X_M-axis parallel to the static magnetic field. This could either be due to a preferred molecular orientation from thermal deposition as expected or an effect wherein orientation selects from a specific spin polarization that contributes more strongly to the EDMR signal than others. To disambiguate these two effects we measure the EDMR response of the device as it is physically rotated within the applied field.

Figure 8 shows the simulated and experimental effects of rotating the host−guest device within the applied field as a function of θ_L. For the simulated spectra at 0° rotation, all molecules are chosen to be oriented with an 11.9° tilt away from the X_M-axis with respect to the applied field. The initial tilt is based on the short tilt axis of the Pc unit cell and as a first-order approximation shows good agreement with experiment. The molecular orientation is only initially constrained at an angle from the X_M-axis, and is otherwise isotropically distributed in the Y_M and Z_M directions.

As the rotation angle increases, the triplet wing features begin to shrink toward the center, as they lose the effect of strong zero field splitting from being oriented along a primary axis. With steeper angles of rotation, the triplet wing peaks begin to not only lose character from the X_M-axis orientation, but begin to gain character in the Y_M and Z_M axes. This causes the wing peaks to rapidly broaden as they lose their primary

https://doi.org/10.1021/acs.jpcc.4c02941
J. Phys. Chem. C XXXX, XXX, XXX−XXX

axis identity, until at steep angles the peaks broaden so substantially they are essentially no longer detectable.

The data acquired via lock-in detection was initially collected with no phase offset, and rephased in post at each angle to minimize the signal amplitude of the out-of-phase component. The raw data set and rephasing procedure is described in the Supporting Information Rephasing of the lock-in data provides a clearer view of processes that may be occurring at different time scales than the primary signal of interest. Here, even when the out-of-phase signal is minimized, the center-field feature remains, meaning the resonant transitions at center-field correspond to kinetic processes occurring at a longer time scale than the outer peaks. This provides strong evidence that at least some fraction of the center-field contribution originates from a process that is fundamentally different from that governing the wing peaks. This is not too surprising, as our analysis before shows that in a highly oriented system all doublet transitions appear within the center-field range, while all triplet transitions appear outside of it. Additionally, a noticeable asymmetry also exists between the left $T_{+\leftrightarrow 0}$ and right $T_{-\leftrightarrow 0}$ peak amplitudes in all scans. This could potentially be due to a consequence of the experimental design, an imbalance in the plus and minus sublevel occupations, or some kind of self-polarizing triplet spin effect originating from the asymmetry of the Hamiltonian.

The triplet wing features in both the raw and rephased lock-in data present only positive contributions to the EDMR. This can now be more accurately described with respect to the triplet-charge interaction. A positive phase EDMR feature corresponds to an increase in conductance, so the triplet sublevel transition must result in a reduction in triplet-charge quenching. We can start with the most commonly proposed mechanism in acene ODMR literature, where the $m_s = 0$ sublevel is presumed to be populated preferentially compared to the $m_s = \pm 1$ sublevels.[82−84] The triplet charge interactions formed in this case are more likely to quench as all $m_s = 0$ interactions result in a spin-allowed quenching. Now when the sublevels are driven under resonance, we provide more $m_s = \pm 1$ character to the triplet-charge interactions, and thus an increase in the spin-forbidden scattering pathway. This then aligns well with the increase of conductance seen in experiment here, as the triplet trap-site occupation lifetime is increased, allowing mobile charges to pass by via triplet trap-filling.[50]

It is also worth mentioning one caveat to the observed peak amplitudes due to experimental design. Rotation of the device in these experiments is achieved via simultaneous rotation of the microwave cavity. In the 0° angle EDMR, the microwave cavity configuration applies a microwave-magnetic field B_1 in the positive Z_L-axis, perpendicular to B_0. The microwave cavity and device then rotate in the X_LZ_L plane along θ_L to orient the device at an angle to the applied field direction. This also rotates the microwave-magnetic field B_1 toward aligning with the static field B_0, which has the downside of reducing the allowedness of transitions with a total spin change of ±1. Thus, in the present experimental setup, this will reduce the amplitude of all of the observed doublet and triplet transitions as a function of rotation angle θ_L. This also explains the apparently increasing baseline noise in the measurements conducted at high rotation angles, as each spectrum is normalized for visibility.

The position of these peaks along the applied field axis also strongly implies the existence of the observed triplet spins localized on the guest Pc as opposed to the host Tc. For triplet spins primarily oriented along the X_M-axis with respect to the substrate, one would expect the positive and negative triplet wing peaks to be split by the elongated zero field splitting parameter D_{zfs}. The separation of the host−guest wing peaks in the standard EDMR configuration is observed to be about 1420 MHz, whereas the previously measured D_{zfs} splitting for Pc is 1395 MHz, and for Tc is 1205 MHz.[79] This is consistent with previous research into these blends that has shown strong evidence of preferential triplet generation and migration onto the lower energy Pc.[31] Both the host tetracene homofission and the heterofission pathway between two unlike acene molecules lead to long-lived isolated triplet spin population among the guest Pc across a wide range of Pc loading.[55]

Based on these arguments, it appears that the dilution of Pc is required to detect isolated triplet spins. In fact, host−guest systems are commonly employed in EPR experiments in order to isolate single molecules in the solid state.[67,85−88] More specifically, neat polycrystalline Pc produces little to no resonant features in low temperature EPR experiments, but does reveal a distinct triplet spectrum when diluted in *p*-terphenyl.[18,19,89−93] The two most commonly mentioned mechanisms in EPR literature that could cause peak attenuation are exciton delocalization and spin−lattice relaxation.[94−98]

Delocalization of excitonic species varies dramatically based on material, with some polymeric species exhibiting exciton delocalization upward of 50 nm, while most organics host an exciton on just one or two molecules.[25,99−104] Triplet exciton species tend to be more tightly bound and more localized than their singlet counterparts, and in the linear acenes tend to be constrained to one molecule at most.[25,100,102,105,106] In high concentration, neighboring molecules would tend to delocalize more, resulting in triplet transitions that are less constrained to the molecular axes and an overall reduction in the effective zero field splitting. On the other hand, spin−lattice relaxation effects are caused primarily via exciton hopping in the high concentration limit.[97,98] Triplet excitons are significantly less mobile than singlets in the linear acenes, but are still able to travel long distances due to considerable lifetimes.[63,94,107−110] In the dilute regime, excitons would tend to be isolated and trapped, drastically reducing the spin−lattice relaxation and increasing the initial polarization caused by SF.

Figure 9 shows the theoretical changes to the Pc EDMR triplet wing peaks as either effect is amplified. Exciton delocalization was simulated by calculating the effective

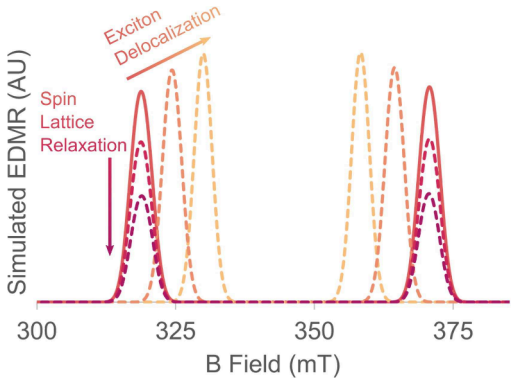

Figure 9. Triplet-only Pc EDMR simulation of two common quantum effects that result in the alteration and eventual disappearance of wing features in high concentrations of the guest molecule.

https://doi.org/10.1021/acs.jpcc.4c02941
J. Phys. Chem. C XXXX, XXX, XXX−XXX

reduction in D_{zfs} and E_{zfs} zero field splitting parameters caused by incorporation of the exciton into 2 and then 4 Pc molecules based on the crystal unit cell. As the triplet exciton is allowed to delocalize, it incorporates neighboring molecules in a way that increases the spherical symmetry of the space it is confined to. This causes the triplet features to collapse toward center-field and become narrower as the similarity of surrounding molecules increases.

Spin−lattice relaxation is a more general term that encompasses the loss of spin polarization from several mechanisms. We argue that the dominant cause of triplet spin−lattice relaxation in high guest concentration is due to exciton hopping via nearest neighbor proximity. Accounting for triplet relaxation, triplet−triplet annihilation, and doublet-triplet quenching, the triplet lifetime in organics ranges from tens of nanoseconds to microseconds. Given a Pc triplet exciton diffusion coefficient of 0.0023 cm^2s^{-1} and a hopping distance of ∼0.7 nm, this gives the average triplet exciton in Pc the opportunity to undergo thousands to millions of hopping events during its lifetime, at a hopping frequency of $k_{hop} = 1.8x10^{12}s^{-1}$ in two dimensions.[111] Figure 10 shows the

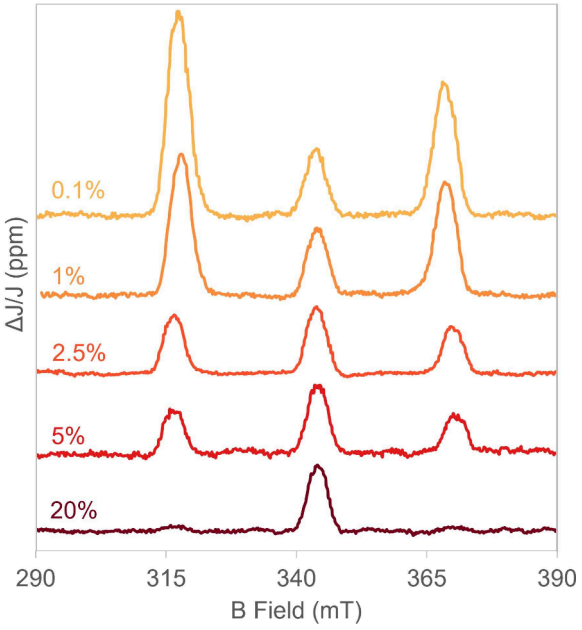

Figure 10. Experimental in-phase EDMR signal of Tc-Pc host−guest devices as a function of % Pc loading. Spectra were taken at the 0° rotational angle and are normalized to the center-field doublet feature.

experimental reduction in triplet EDMR wing peak amplitude as a function of increasing guest Pc concentration. In all spectra, the wing peak positions vary at most by 2 mT, implying that the spin−lattice relaxation effect is the dominant mechanism with increasing guest concentration and not exciton delocalization. The lack of exciton delocalization in the linear acenes is also reflected in the host−guest absorption spectra presented in the Supporting Information This experiment serves as a confirmation of the exciton localization in this system, which is not always observed in resonance experiments of other organic semiconductors.

From these results we can expand further on the reduction in spin polarization and model the spin−lattice relaxation in terms of the ratio of isolated to mobile triplets. In the acenes, even one hopping event can result in a spin reorientation, due to the alternating herringbone structure of the crystal lattice. Not all hopping events result in a reorientation, but the diffusion coefficients are known to be highest in the a-b plane of the crystal lattice where these herringbone hops occur.[78,111,112] As an approximation, we choose to model the spin−lattice relaxation effect by calculating the amount of guest molecules that are considered fully isolated and cannot undergo even one hopping event as a function of guest loading. The Poisson distribution can be used to model the random distribution of guest molecules in a host matrix, and is given by

$$P(k; N) = (N^k e^{-N})/k! \quad (15)$$

which calculates the probability P of observing k distinct events given an average number of total events N. The probability that a guest molecule is isolated can then be calculated when k is set to 0, where N represents the available neighbors:

$$P(k = 0; N) = e^{-N} = e^{-\rho 4/3\pi\epsilon^3} \quad (16)$$

Here, ρ is the point density of acene molecules and the search radius for the nearest molecule is defined by a sphere of radius ϵ. Figure 11 shows a comparison of the simulated

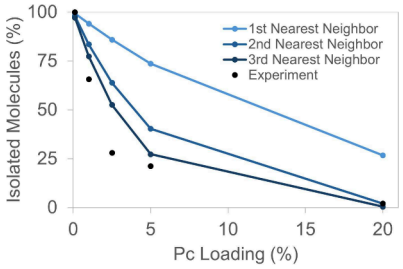

Figure 11. Simulation of isolated guest Pc molecules randomly distributed in a host Tc matrix as a function of guest loading. Molecules are considered to be isolated when the only nearest neighbors are host molecules. The first nearest neighbor is considered to be the closest molecule on the short axis of the triclinic unit cell, where the third nearest neighbor would be across the full diagonal of one unit cell.

number of isolated Pc guest molecules as ϵ is increased to allow further nearest neighbors. As a comparison, we also show the normalized sum of the integrated wing peaks from Figure 10 as a function of Pc loading. The experimental data set does not align perfectly with simulation, but the overall trend aligns remarkably well just with the predicted isolation of randomly distributed guest molecules. Of course there remains a sizable uncertainty in the acene deposition rates of the thin films, and there could be several experimental factors that would account for the discrepancy. It is possible that hopping events can occur between guest molecules separated by multiple hosts, as the tunneling barrier between non-nearest neighbor Pc molecules is not very large compared with a *p*-terphenyl or phenacene host. It is also possible that exciton and charge dynamics are altered as the Tc lattice and associated crystallites are distorted as the Pc fraction increases.[57] And last, triplet−triplet annihilation effects could bridge this gap between theory and experiment, as we do not account for guest triplet annihilation as the interaction frequency is predicted to be several orders of magnitude lower than that of the triplet-charge interactions.

From these key discoveries, we can draw several conclusions about the observation of triplet features among the different linear acenes as a function of detection scheme. In optically

https://doi.org/10.1021/acs.jpcc.4c02941
J. Phys. Chem. C XXXX, XXX, XXX−XXX

detected measurements, triplet features arise from the kinetic balance between the correlated triplet pair state and the first excited singlet state. Triplet spins born via singlet fission are initially spin-polarized, and in the correlated triplet pair configuration can either separate or undergo triplet fusion back to a ground state and first excited singlet. In photoluminescence-detected ODMR measurements (PLDMR), the radiative transition from the singlet is the transition being monitored, and so there must be a sufficient balance between singlet fission and triplet fusion for the triplet spins to affect the measurement. Therefore, the cutoff point to observe triplet PLDMR in the linear acenes occurs between tetracene, where the SF reaction is endothermic (0.18 eV), and pentacene, where the SF reaction is exothermic (−0.11 eV).[113,114] The correlated triplet pair in tetracene boasts a sufficiently short lifetime around 1 ns, compared to the spin−lattice relaxation time of around 10−100 ns, meaning driving triplet sublevel transitions within the pair modulates the singlet occupation, and thus produces an ODMR signal.[64] On the other hand, the SF in pentacene is so energetically downhill that nearly all exciton species favor the triplet configuration and no change in the singlet occupation is detected via PLDMR.[85,111]

In electrically detected schemes, the triplet features arise from a separate mechanism and no longer rely on the excited singlet state to be detectable. Here, triplet species affect the conduction by occupying trap sites, so interactions that affect the average trapped triplet occupation, like triplet-charge interactions are detectable. Resonant transitions will now only appear in systems where the triplet-charge interaction rate occurs on a faster time scale than other triplet relaxation pathways like triplet−triplet annihilation or exciton hopping. While it is still not abundantly clear why triplet species in crystalline anthracene are electrically detectable compared to the longer acenes, some contributing factors stand out. Singlet fission in crystalline anthracene is much less favored due to the endothermic nature of the reaction (0.53 eV), and thus triplet density at equilibrium remains low. Lifetimes of triplet-doublet interactions in crystalline anthracene (2 ns), are reportedly lower than those observed in crystalline tetracene (7 ns).[54,58] It is possible the faster triplet-doublet interaction rate in anthracene out-competes the other triplet relaxation pathways, and in the longer acenes the high triplet density and hopping mobility contributes to triplet quenching and triplet relaxation on shorter time scales. Resulting in the cutoff point where triplet features are electrically detectable in the linear acene series to occur between anthracene and tetracene.

The host−guest system presented herein provides an opportunity to bypass the triplet detection limitations in magnetic resonance experiments observed in the neat acenes. Unlike Pc, the host Tc loses SF efficiency as a function of applied field due to its endothermic nature. The host−guest system necessarily possesses a lower triplet density compared to neat Pc, and triplets that are generated under photoexcitation are primarily harbored on the guest Pc. The decrease in exciton mobility now allows the triplet spins to retain their original polarization from the SF process. These effects explain the minimal MC observed in the host−guest system, as triplet-charge interactions are drastically reduced in the high-field limit. The interactions that remain are however now electrically detectable, thanks to the SF process preferentially populating the $m_s = 0$ triplet sublevel. Under resonant conditions, the $m_s = \pm 1$ sublevels are now in relatively higher concentration, and so triplet-charge interactions produce more scattering states and result in a reduction of quenched triplets. The higher average trapped triplet lifetime results in more efficient trap-blocking, an increase in conductance, and a positive phase EDMR signal.

CONCLUSIONS

We report electrically detected magnetic resonance studies of both neat acene and codeposited host−guest acene systems aimed at discovering whether electrical detection of the exciton spin state in these systems can be a useful platform for molecular quantum information applications. The host−guest architecture of pentacene in tetracene shows the first reported EDMR spectrum of a triplet-state on pentacene, confirming the value of electrical detection. The sign of the triplet transitions are consistent with our previously reported trap-filling model of organic magnetoconductance, and the spectra show a high degree of molecular orientation. By rotating the device with respect to the applied field, we were able to confirm the crystallographic orientation bias in the thin film through EDMR, and separate the contributions from doublet and triplet transitions. However, it remains unclear whether an observed asymmetry in the intensity of the plus and minus triplet transitions is due to an experimental complication or if this is a self-polarizing effect caused by the asymmetry of the underlying Hamiltonian. Future work on the nature of this apparent self-polarization could provide valuable direction toward the initialization of molecular quantum systems.

We find the triplet sublevel transitions diminish and ultimately vanish as the concentration of pentacene guest molecules increases, without any apparent shift in their field positions. This behavior explains the absence of triplet transitions in previous EDMR studies of tetracene and pentacene and shows that spin−lattice relaxation is the primary driver. From this experiment we find no evidence of exciton delocalization, which has been used to explain the disappearance of features in other organic semiconductor resonance experiments. We propose that exciton hopping events are the primary cause of this efficient relaxation, and provide a model based on the declining probability of finding fully isolated guest molecules in the film as their concentration increases. This ensemble host−guest system displays the primary requirements needed for quantum information applications and could feasibly be incorporated in a room temperature quantum sensing protocol. We propose future work focused on using the singlet fission phenomenon to accomplish the spin initialization and a pulsed-EDMR scheme to realize the electrical manipulation and readout of these spins in a simple useful quantum protocol. Computing applications would ultimately require scaling to single molecule tunnel junctions,[12,13] and implementing a mechanism of establishing remote entanglement.[15] Overall, we believe the results presented here resolve the discrepancy in previously reported magnetic resonance spectra of the different acenes as a function of detection scheme, and pave the way for electrical readout of future molecular systems by means of enhanced triplet exciton detection in solid state host−guest systems.

ASSOCIATED CONTENT

Supporting Information

The Supporting Information is available free of charge at https://pubs.acs.org/doi/10.1021/acs.jpcc.4c02941.

Optical characterization, photoconductivity measurements, full MC and EDMR data of neat and host−

https://doi.org/10.1021/acs.jpcc.4c02941
J. Phys. Chem. C XXXX, XXX, XXX−XXX

guest devices, lock-in rephasing procedure, cryogenic EDMR, magnetic resonance modeling, and isolated triplet modeling (PDF)

AUTHOR INFORMATION

Corresponding Author

Obadiah G. Reid − *University of Colorado Boulder, Renewable and Sustainable Energy Institute, Boulder, Colorado 80309, United States; National Renewable Energy Laboratory, Golden, Colorado 80401, United States;* orcid.org/0000-0003-0646-3981; Email: obadiah.reid@colorado.edu

Authors

Taylor W. Wagner − *Colorado School of Mines, Department of Physics, Golden, Colorado 80401, United States; National Renewable Energy Laboratory, Golden, Colorado 80401, United States;* orcid.org/0000-0003-4935-5083

Paul Niyonkuru − *Colorado School of Mines, Department of Physics, Golden, Colorado 80401, United States*

Justin C. Johnson − *National Renewable Energy Laboratory, Golden, Colorado 80401, United States; University of Colorado Boulder, Renewable and Sustainable Energy Institute, Boulder, Colorado 80309, United States;* orcid.org/0000-0002-8874-6637

Complete contact information is available at: https://pubs.acs.org/10.1021/acs.jpcc.4c02941

Notes

The authors declare no competing financial interest.

ACKNOWLEDGMENTS

This work was authored in part by the National Renewable Energy Laboratory, operated by Alliance for Sustainable Energy, LLC, for the U.S. Department of Energy (DOE) under contract no. DE-AC36-08GO28308. Funding was provided by the Laboratory Directed Research and Development (LDRD) Program at NREL. T.W.W. acknowledges funding from the NSF NRT program DGE-2125899. The views expressed in the article do not necessarily represent the views of the DOE or the U.S. Government. The U.S. government retains and the publisher, by accepting the article for publication, acknowledges that the U.S. Government retains a nonexclusive, paid-up, irrevocable, worldwide license to publish or reproduce the published form of this work, or allow others to do so, for U.S. government purposes. We thank L. Romanetz for useful discussions and assistance in obtaining cryogenic data. We thank A. Phillips for useful discussions and assistance with experimental design.

REFERENCES

(1) Sanvito, S. Molecular spintronics. *Chem. Soc. Rev.* **2011**, *40*, 3336−3355.

(2) Geng, R.; Luong, H. M.; Daugherty, T. T.; Hornak, L.; Nguyen, T. D. A review on organic spintronic materials and devices: II. Magnetoresistance in organic spin valves and spin organic light emitting diodes. *Journal of Science: Advanced Materials and Devices* **2016**, *1*, 256−272.

(3) Wang, S.-J.; Venkateshvaran, D.; Mahani, M. R.; Chopra, U.; McNellis, E. R.; Di Pietro, R.; Schott, S.; Wittmann, A.; Schweicher, G.; Cubukcu, M.; et al. Long spin diffusion lengths in doped conjugated polymers due to enhanced exchange coupling. *Nature Electronics* **2019**, *2*, 98−107.

(4) Filidou, V.; Simmons, S.; Karlen, S. D.; Giustino, F.; Anderson, H. L.; Morton, J. J. L. Ultrafast entangling gates between nuclear spins using photoexcited triplet states. *Nat. Phys.* **2012**, *8*, 596−600.

(5) Akhtar, W.; Filidou, V.; Sekiguchi, T.; Kawakami, E.; Itahashi, T.; Vlasenko, L.; Morton, J. J. L.; Itoh, K. M. Coherent Storage of Photoexcited Triplet States Using Si-29 Nuclear Spins in Silicon. *Phys. Rev. Lett.* **2012**, *108*, 097601.

(6) Filidou, V.; Mamone, S.; Simmons, S.; Karlen, S. D.; Anderson, H. L.; Kay, C. W. M.; Bagno, A.; Rastrelli, F.; Murata, Y.; Komatsu, K.; et al. Probing the C-60 triplet state coupling to nuclear spins inside and out. *Philosophical Transactions of the Royal Society a- Mathematical Physical and Engineering Sciences* **2013**, *371*, 20120475.

(7) Reid, O. G.; Johnson, J. C.; Eaves, J. D.; Damrauer, N. H.; Anthony, J. E. Molecular Control of Triplet-Pair Spin Polarization and Its Optoelectronic Magnetic Resonance Probes. *Acc. Chem. Res.* **2024**, *57*, 59−69.

(8) Siyushev, P.; Nesladek, M.; Bourgeois, E.; Gulka, M.; Hruby, J.; Yamamoto, T.; Trupke, M.; Teraji, T.; Isoya, J.; Jelezko, F. Photoelectrical imaging and coherent spin-state readout of single nitrogen-vacancy centers in diamond. *Science* **2019**, *363*, 728−731.

(9) Kagan, C. R.; Bassett, L. C.; Murray, C. B.; Thompson, S. M. Colloidal Quantum Dots as Platforms for Quantum Information Science. *Chem. Rev.* **2021**, *121*, 3186−3233.

(10) Russ, M.; Burkard, G. Three-electron spin qubits. *J. Phys.: Condens. Matter* **2017**, *29*, 393001.

(11) Koppens, F. H. L.; Buizert, C.; Tielrooij, K. J.; Vink, I. T.; Nowack, K. C.; Meunier, T.; Kouwenhoven, L. P.; Vandersypen, L. M. K. Driven coherent oscillations of a single electron spin in a quantum dot. *Nature* **2006**, *442*, 766−771.

(12) Vincent, R.; Klyatskaya, S.; Ruben, M.; Wernsdorfer, W.; Balestro, F. Electronic read-out of a single nuclear spin using a molecular spin transistor. *Nature* **2012**, *488*, 357−360.

(13) Thiele, S.; Balestro, F.; Ballou, R.; Klyatskaya, S.; Ruben, M.; Wernsdorfer, W. Electrically driven nuclear spin resonance in single-molecule magnets. *Science* **2014**, *344*, 1135−1138.

(14) Yu, C.-J.; von Kugelgen, S.; Laorenza, D. W.; Freedman, D. E. A Molecular Approach to Quantum Sensing. *ACS Central Science* **2021**, *7*, 712−723.

(15) Borjans, F.; Croot, X. G.; Mi, X.; Gullans, M. J.; Petta, J. R. Resonant microwave-mediated interactions between distant electron spins. *Nature* **2020**, *577*, 195−198.

(16) Rugg, B. K.; Smyser, K. E.; Fluegel, B.; Chang, C. H.; Thorley, K. J.; Parkin, S.; Anthony, J. E.; Eaves, J. D.; Johnson, J. C. Triplet-Pair Spin Signatures from Macroscopically Aligned Heteroacenes in an Oriented Single Crystal. *Proceedings of the National Academy of Sciences* **2022**, *119*, e2201879119.

(17) Dill, R. D.; Joshi, G.; Thorley, K. J.; Anthony, J. E.; Fluegel, B.; Johnson, J. C.; Reid, O. G. Near-Infrared Absorption Features of Triplet-Pair States Assigned by Photoinduced-Absorption- Detected Magnetic Resonance. *J. Phys. Chem. Lett.* **2023**, *14*, 2387−2394.

(18) Lubert-Perquel, D.; Szumska, A. A.; Azzouzi, M.; Salvadori, E.; Ruloff, S.; Kay, C. M. W.; Nelson, J.; Heutz, S. Structure Dependence of Kinetic and Thermodynamic Parameters in Singlet Fission Processes. *J. Phys. Chem. Lett.* **2020**, *11*, 9557−9565.

(19) Lubert-Perquel, D.; Salvadori, E.; Dyson, M.; Stavrinou, P. N.; Montis, R.; Nagashima, H.; Kobori, Y.; Heutz, S.; Kay, C. W. M. Identifying triplet pathways in dilute pentacene films. *Nat. Commun.* **2018**, *9*, 4222.

(20) Joshi, G.; Dill, R. D.; Thorley, K. J.; Anthony, J. E.; Reid, O. G.; Johnson, J. C. Optical readout of singlet fission biexcitons with photoluminescence detected magnetic resonance. *J. Chem. Phys.* **2022**, *157*, 164702.

(21) Pace, N. A.; Zhang, W.; Arias, D. H.; McCulloch, I.; Rumbles, G.; Johnson, J. C. Controlling Long-Lived Triplet Generation from Intramolecular Singlet Fission in the Solid State. *J. Phys. Chem. Lett.* **2017**, *8*, 6086−6091.

(22) Sellies, L.; Spachtholz, R.; Bleher, S.; Eckrich, J.; Scheuerer, P.; Repp, J. Single-molecule electron spin resonance by means of atomic force microscopy. *Nature* **2023**, *624*, 64−68.

(23) Merrifield, R. E. Magnetic effects on triplet exciton interactions. *Pure Appl. Chem.* **1971**, *27*, 481−498.
(24) Yarmus, L.; Rosenthal, J.; Chopp, M. EPR of triplet excitions in tetracene crystals: spin polarization and the role of singlet exciton fission. *Chem. Phys. Lett.* **1972**, *16*, 477−481.
(25) Zimmerman, P. M.; Bell, F.; Casanova, D.; Head-Gordon, M. Mechanism for Singlet Fission in Pentacene and Tetracene: From Single Exciton to Two Triplets. *J. Am. Chem. Soc.* **2011**, *133*, 19944−19952.
(26) Piland, G. B.; Burdett, J. J.; Dillon, R. J.; Bardeen, C. J. Singlet Fission: From Coherences to Kinetics. *J. Phys. Chem. Lett.* **2014**, *5*, 2312−2319.
(27) Aryanpour, K.; Shukla, A.; Mazumdar, S. Theory of Singlet Fission in Polyenes, Acene Crystals, and Covalently Linked Acene Dimers. *J. Phys. Chem. C* **2015**, *119*, 6966−6979.
(28) Wolf, H. C. In *Solid State Physics*, Seitz, F., Turnbull, D., Eds.; Academic Press: 1959; Vol. *9*, pp 1−81.
(29) Avakian, P.; Abramson, E.; Kepler, R. G.; Caris, J. C. Indirect Observation of Singlet-Triplet Absorption in Anthracene Crystals. *J. Chem. Phys.* **1963**, *39*, 1127−1128.
(30) Tomkiewicz, Y.; Groff, R. P.; Avakian, P. Spectroscopic Approach to Energetics of Exciton Fission and Fusion in Tetracene Crystals. *J. Chem. Phys.* **1971**, *54*, 4504−4507.
(31) Geacintov, N. E.; Burgos, J.; Pope, M.; Strom, C. Heterofission of pentacene excited singlets in pentacene-doped tetracene crystals. *Chem. Phys. Lett.* **1971**, *11*, 504−508.
(32) Sebastian, L.; Weiser, G.; Bässler, H. Charge transfer transitions in solid tetracene and pentacene studied by electroabsorption. *Chem. Phys.* **1981**, *61*, 125−135.
(33) Van Strien, A. J.; Schmidt, J. An EPR study of the triplet state of pentacene by electron spin-echo techniques and laser flash excitation. *Chem. Phys. Lett.* **1980**, *70*, 513−517.
(34) Wang, L.; Wu, Y.; Liu, Y.; Wang, L.; Yao, J.; Fu, H. Morphology independent triplet formation in pentalene films: Singlet fission as the triplet formation mechanism. *J. Chem. Phys.* **2019**, *151*, 124701.
(35) Wang, L.; Bai, S.; Wu, Y.; Liu, Y.; Yao, J.; Fu, H. Revealing the Nature of Singlet Fission under the Veil of Internal Conversion. *Angew. Chem., Int. Ed.* **2020**, *59*, 2003−2007.
(36) Lukman, S.; Musser, A. J.; Chen, K.; Athanasopoulos, S.; Yong, C. K.; Zeng, Z.; Ye, Q.; Chi, C.; Hodgkiss, J. M.; Wu, J.; et al. Tuneable Singlet Exciton Fission and Triplet-Triplet Annihilation in an Orthogonal Pentacene Dimer. *Adv. Funct. Mater.* **2015**, *25*, 5452−5461.
(37) Zirzlmeier, J.; Lehnherr, D.; Coto, P. B.; Chernick, E. T.; Casillas, R.; Basel, B. S.; Thoss, M.; Tykwinski, R. R.; Guldi, D. M. Singlet fission in pentacene dimers. *Proc. Natl. Acad. Sci. U.S.A.* **2015**, *112*, 5325−5330.
(38) Smyser, K. E.; Eaves, J. D. Singlet fission for quantum information and quantum computing: the parallel JDE model. *Sci. Rep.* **2020**, *10*, 18480.
(39) Dill, R. D.; Smyser, K. E.; Rugg, B. K.; Damrauer, N. H.; Eaves, J. D. Entangled spin-polarized excitons from singlet fission in a rigid dimer. *Nat. Commun.* **2023**, *14*, 1180.
(40) Kawashima, Y.; Hamachi, T.; Yamauchi, A.; Nishimura, K.; Nakashima, Y.; Fujiwara, S.; Kimizuka, N.; Ryu, T.; Tamura, T.; Saigo, M.; et al. Singlet fission as a polarized spin generator for dynamic nuclear polarization. *Nat. Commun.* **2023**, *14*, 1056.
(41) Johnson, J. C. Open questions on the photophysics of ultrafast singlet fission. *Communications Chemistry* **2021**, *4*, 85.
(42) Desai, P.; Shakya, P.; Kreouzis, T.; Gillin, W. P.; Morley, N. A.; Gibbs, M. R. J. Magnetoresistance and efficiency measurements of Alq3-based OLEDs. *Phys. Rev. B* **2007**, *75*, 094423.
(43) Cox, M.; Janssen, P.; Zhu, F.; Koopmans, B. Traps and trions as origin of magnetoresistance in organic semiconductors. *Phys. Rev. B* **2013**, *88*, 035202.
(44) Zhang, T.; Holford, D. F.; Gu, H.; Kreouzis, T.; Zhang, S.; Gillin, W. P. Hole-exciton interaction induced high field decay of magneto-electroluminescence in Alq3-based organic light-emitting diodes at room temperature. *Appl. Phys. Lett.* **2016**, *108*, 023303.
(45) Howard, I. A.; Hodgkiss, J. M.; Zhang, X.; Kirov, K. R.; Bronstein, H. A.; Williams, C. K.; Friend, R. H.; Westenhoff, S.; Greenham, N. C. Charge Recombination and Exciton Annihilation Reactions in Conjugated Polymer Blends. *J. Am. Chem. Soc.* **2010**, *132*, 328−335.
(46) Schellekens, A. J.; Wagemans, W.; Kersten, S. P.; Bobbert, P. A.; Koopmans, B. Microscopic modeling of magneticfield effects on charge transport in organic semiconductors. *Phys. Rev. B* **2011**, *84*, 075204.
(47) Gu, H.; Zhang, X.; Wei, H.; Huang, Y.; Wei, S.; Guo, Z. An overview of the magnetoresistance phenomenon in molecular systems. *Chem. Soc. Rev.* **2013**, *42*, 5907−5943.
(48) Peng, Q.; Chen, P.; Li, F. Experimental investigation on the origin of magneto-conductance and magnetoelectroluminescence in organic light emitting devices. *Synth. Met.* **2013**, *173*, 31−34.
(49) Gobbi, M.; Orgiu, E. The rise of organic magnetoresistance: materials and challenges. *Journal of Materials Chemistry C* **2017**, *5*, 5572−5580.
(50) Wagner, T. W.; Johnson, J. C.; Reid, O. G. Trap-Filling Magnetoconductance as an Initialization and Readout Mechanism of Triplet Exciton Spins. *J. Phys. Chem. Lett.* **2022**, *13*, 9895−9902.
(51) Cox, M.; van der Heijden, E. H. M.; Janssen, P.; Koopmans, B. Investigating the influence of traps on organic magnetoresistance by molecular doping. *Phys. Rev. B* **2014**, *89*, 085201.
(52) Chernick, E. T.; Casillas, R.; Zirzlmeier, J.; Gardner, D. M.; Gruber, M.; Kropp, H.; Meyer, K.; Wasielewski, M. R.; Guldi, D. M.; Tykwinski, R. R. Pentacene Appended to a TEMPO Stable Free Radical: The Effect of Magnetic Exchange Coupling on Photoexcited Pentacene. *J. Am. Chem. Soc.* **2015**, *137*, 857−863.
(53) Arias, D. H.; Ryerson, J. L.; Cook, J. D.; Damrauer, N. H.; Johnson, J. C. Polymorphism influences singlet fission rates in tetracene thin films. *Chemical Science* **2016**, *7*, 1185−1191.
(54) Barhoumi, T.; Romdhane, S.; Ben Fredj, A.; Henia, F.; Bouchriha, H. Photoconductivity detected magnetic resonance (PDMR) in crystalline tetracene. *European Physical Journal B - Condensed Matter and Complex Systems* **2003**, *34*, 143−153.
(55) Zeiser, C.; Moretti, L.; Lepple, D.; Cerullo, G.; Maiuri, M.; Broch, K. Singlet Heterofission in Tetracene-Pentacene Thin-Film Blends. *Angew. Chem., Int. Ed.* **2020**, *59*, 19966−19973.
(56) Tsague, L. F.; Ejuh, G. W.; Ndjaka, J. M. B. Computational determination of the electronic structure, optoelectronics, thermodynamics and nonlinear optical properties of undoped and doped pentacene and tetracene. *Optical and Quantum Electronics* **2022**, *54*, 579.
(57) Unger, F.; Lepple, D.; Asbach, M.; Craciunescu, L.; Zeiser, C.; Kandolf, A. F.; Fišer, Z.; Hagara, J.; Hagenlocher, J.; Hiller, S.; et al. Optical Absorption Properties in Pentacene/Tetracene Solid Solutions. *J. Phys. Chem. A* **2024**, *128*, 747−760.
(58) Bouchriha, H.; Monge, J. L.; Ern, V.; Romdhane, S.; Fredj, A. B. Perturbation par une puissance micro-onde de l'interaction triplet-doublet dans les cristaux moléculaires. Application à la photoconductivité de l'anthracène. *Journal de Physique I* **1993**, *3*, 203−219.
(59) Barhoumi, T.; Monge, J. L.; Bouchriha, H. Application of the short and long consecutive pairs model tothe tripletdoublet interaction in molecular crystals. *European Physical Journal B* **2010**, *77*, 453−458.
(60) Fukuda, K.; Asakawa, N. Development of multi-frequency ESR/EDMR system using a rectangular cavity equipped with waveguide window. *Rev. Sci. Instrum.* **2016**, *87*, 113106.
(61) Fukuda, K.; Asakawa, N. Spindependent electrical conduction in a pentacene Schottky diode explored by electrically detected magnetic resonance. *J. Phys. D: Appl. Phys.* **2017**, *50*, 055102.
(62) Fukuda, K.; Asakawa, N. Angular- Dependent EDMR Linewidth for Spin- Dependent Space-Charge-Limited Conduction in a Polycrystalline Pentacene. *Frontiers in Materials* **2017**, *4*, DOI: 10.3389/fmats.2017.00024.
(63) Kato, K.; Teki, Y. Photogenerated carrier dynamics of TIPS-pentacene films as studied by photocurrent and electrically detected magnetic resonance. *Phys. Chem. Chem. Phys.* **2021**, *23*, 6361−6369.

(64) Barhoumi, T.; Henia, F.; Romdhane, S.; Monge, J. L.; Mejatty, M.; Bouchriha, H. Saturation of the ODMR effect on singlet exciton induced emission in molecular crystals: Application to crystalline tetracene. *European Physical Journal B - Condensed Matter and Complex Systems* **2004**, *38*, 395−402.
(65) Barhoumi, T.; Monge, J. L.; Mejatty, M.; Bouchriha, H. Short and long consecutive pairs model in the interpretation of MFEand F-ODMR experiments in molecular crystals. *European Physical Journal B* **2007**, *59*, 167−172.
(66) Biskup, T. Structure-Function Relationship of Organic Semiconductors: Detailed Insights From Time-Resolved EPR Spectroscopy. *Frontiers in Chemistry* **2019**, *7*, DOI: 10.3389/fchem.2019.00010.
(67) Braun, F.; Scharff, T.; Grünbaum, T.; Schmid, E.; Bange, S.; Mkhitaryan, V.; Lupton, J. Polaron-induced upconversion from triplets to singlets: Fluorescence- and phosphorescenceresolved optically detected magnetic resonance of OLEDs. *Physical Review Applied* **2023**, *20*, 044076.
(68) Bertens, K.; Fan, J. Z.; Biondi, M.; Rasouli, A. S.; Lee, S.; Li, P.; Sun, B.; Hoogland, S.; García de Arquer, F. P.; Lu, Z.-H.; et al. Colloidal Quantum Dot Solar Cell Band Alignment using Two- Step Ionic Doping. *ACS Materials Letters* **2020**, *2*, 1583−1589.
(69) Biondi, M.; Choi, M.-J.; Lee, S.; Bertens, K.; Wei, M.; Kirmani, A. R.; Lee, G.; Kung, H. T.; Richter, L. J.; Hoogland, S.; et al. Control Over Ligand Exchange Reactivity in Hole Transport Layer Enables High-Efficiency Colloidal Quantum Dot Solar Cells. *ACS Energy Letters* **2021**, *6*, 468−476.
(70) Lee, T. H.; Lai, K. M.; Leung, L. M. Hole-limiting conductive vinyl copolymers for AlQ3-based OLED applications. *Polymer* **2009**, *50*, 4602−4611.
(71) Rana, O.; Srivastava, R.; Grover, R.; Chauhan, G.; Bawa, S. S.; Zulfequar, M.; Husain, M.; Kamalasanan, M. N. Charge Transport Study of 2,2',7,7'-Tetrakis(N,N-di-4- methoxyphenyl amino)-9,9'-spirobifluorene Using Impedance Spectroscopy. *Jpn. J. Appl. Phys.* **2011**, *50*, 061601.
(72) Röhr, J. A.; Moia, D.; Haque, S. A.; Kirchartz, T.; Nelson, J. Exploring the validity and limitations of the Mott-Gurney law for charge-carrier mobility determination of semiconducting thin-films. *J. Phys.: Condens. Matter* **2018**, *30*, 105901.
(73) Mermer, ö.; Veeraraghavan, G.; Francis, T. L.; Sheng, Y.; Nguyen, D. T.; Wohlgenannt, M.; Köhler, A.; Al-Suti, M. K.; Khan, M. S. Large magnetoresistance in nonmagnetic Pi-conjugated semiconductor thin film devices. *Phys. Rev. B* **2005**, *72*, 205202.
(74) Bloom, F. L.; Wagemans, W.; Kemerink, M.; Koopmans, B. Separating Positive and Negative Magnetoresistance in Organic Semiconductor Devices. *Phys. Rev. Lett.* **2007**, *99*, 257201.
(75) Bergeson, J. D.; Prigodin, V. N.; Lincoln, D. M.; Epstein, A. J. Inversion of Magnetoresistance in Organic Semiconductors. *Phys. Rev. Lett.* **2008**, *100*, 067201.
(76) Jia, W.; Chen, Q.; Chen, Y.; Chen, L.; Xiong, Z. Magneto-conductance characteristics of trapped triplet-polaron and triplet-trapped polaron interactions in anthracene-based organic light emitting diodes. *Phys. Chem. Chem. Phys.* **2016**, *18*, 30733−30739.
(77) Chen, L.; Jia, W.; Lan, Z.; Tang, X.; Zhu, F.; Xiong, Z. Tuning the polarity of organic magnetic field effects in polymer light-emitting diodes by incorporating a colloidal quantum dots thin layer. *Org. Electron.* **2018**, *55*, 165−169.
(78) Lubert-Perquel, D.; Kim, D. K.; Robaschik, P.; Kay, C. W. M.; Heutz, S. Growth, morphology and structure of mixed pentacene films. *Journal of Materials Chemistry C* **2019**, *7*, 289−296.
(79) Yang, T.-C.; Sloop, D. J.; Weissman, S. I.; Lin, T.-S. Zero-field magnetic resonance of the photo-excited triplet state of pentacene at room temperature. *J. Chem. Phys.* **2000**, *113*, 11194−11201.
(80) Van der Est, A.; Asano-Someda, M.; Ragogna, P.; Kaizu, Y. Light-Induced Electron Spin Polarization of a Weakly Coupled TripletDoublet Spin Pair in a Covalently Linked Porphyrin Dimer. *J. Phys. Chem. A* **2002**, *106*, 8531−8542.
(81) Beentjes, C. H. L. *Quadrature on a Spherical Surface*; 2010 Mathematics Subject Classification. 65D30,65D32. Mathematical Institute; University of Oxford, Oxford, U.K., 2015; p 15.
(82) Clarke, R. H.; Frank, H. A. Triplet state radiationless transitions in polycyclic hydrocarbons. *J. Chem. Phys.* **1976**, *65*, 39−47.
(83) Clarke, R. H.; Hayes, J. M.; Hofeldt, R. H. Determination of triplet state intersystem crossing rate constants by microwave induced triplet-triplet absorption in organic molecules. *Journal of Magnetic Resonance (1969)* **1974**, *13*, 68−75.
(84) Chiha, P. A.; Clarke, R. H. Tripletstate intersystem crossing rates from optically detected magnetic resonance spectroscopy. *Journal of Magnetic Resonance (1969)* **1978**, *29*, 535−543.
(85) Ong, J. L.; Sloop, D. J.; Lin, T. S. Temperature dependence studies of the paramagnetic properties of the photoexcited triplet states of pentacene in pterphenyl, benzoic acid, and naphthalene crystals. *J. Phys. Chem.* **1993**, *97*, 7833−7838.
(86) Kilin, S. Y.; Nizovtsev, A. P.; Berman, P. R.; von Borczyskowski, C.; Wrachtrup, J. Theory of non-Markovian relaxation of single triplet electron spins using time- and frequency-domain magnetic resonance spectroscopy measured via optical fluorescence: Application to single pentacene molecules in crystalline p-terphenyl. *Phys. Rev. B* **1998**, *58*, 8997−9017.
(87) Batagin-Neto, A.; Gómez, J. A.; Castro, F. A.; Nüesch, F.; Zuppiroli, L.; Graeff, C. F. O. Photonics and Optoelectronics Meetings (POEM) 2011: Optoelectronic Devices and Integration. *Proc. SPIE* **2012**, *8333*, 317−323.
(88) Tedlla, B. Z.; Zhu, F.; Cox, M.; Drijkoningen, J.; Manca, J.; Koopmans, B.; Goovaerts, E. Understanding Triplet Formation Pathways in Bulk Heterojunction Polymer:Fullerene Photovoltaic Devices. *Adv. Energy Mater.* **2015**, *5*, 1401109.
(89) Lang, J.; Sloop, D. J.; Lin, T.-S. Dynamics of p-Terphenyl Crystals at the Phase Transition Temperature: A Zero- Field EPR Study of the Photoexcited Triplet State of Pentacene in p-Terphenyl Crystals. *J. Phys. Chem. A* **2007**, *111*, 4731−4736.
(90) Yago, T.; Link, G.; Kothe, G.; Lin, T.-S. Pulsed electron nuclear double resonance studies of the photoexcited triplet state of pentacene in p-terphenyl crystals at room temperature. *J. Chem. Phys.* **2007**, *127*, 114503.
(91) Schmidt, J. *10th International Symposium on Nanostructures: Physics and Technology*; SPIE: 2003; Vol. *5023*, pp 127−133.
(92) Köhler, J.; Brouwer, A. C. J.; Groenen, E. J. J.; Schmidt, J. Fluorescence detection of single molecule magnetic resonance for pentacene in p-terphenyl. The hyperfine interaction of a single triplet spin with a single 13C nuclear spin. *Chem. Phys. Lett.* **1994**, *228*, 47−52.
(93) Köhler, J. Magnetic resonance of a single molecular spin. *Phys. Rep.* **1999**, *310*, 261−339.
(94) Shushin, A. I. Manifestation of Texciton migration in the kinetics of singlet fission in organic semiconductors. *Chem. Phys. Lett.* **2017**, *678*, 283−288.
(95) Popescu, F. F.; Martinelli, M.; Massa, C. A.; Pardi, L. A.; Bercu, V. Delocalization of spin projection in weak exchange linear chains, evidenced by multi-frequency HF-EPR spectroscopy. *Magn. Reson. Chem.* **2005**, *43*, S215−S220.
(96) Yin, S.; Xie, S. J.; Gao, K.; Wang, X. R. Temperature effect on spin relaxation in organic semiconductors. *Synth. Met.* **2013**, *165*, 35−39.
(97) Tarasov, V. V.; Zoriniants, G. E.; Shushin, A. I.; Triebel, M. M. The role of spin-lattice relaxation in magnetic field effects on the luminescence of amorphous and polycrystalline rubrene films. *Chem. Phys. Lett.* **1997**, *267*, 58−64.
(98) Konyaev, S. N.; Shushin, A. I.; Kolesnikova, L. I.; Tribel, M. M.; Frankevich, E. L. Fluorescence- Detected Low Field Resonances in T-T Annihilation in the A-TCNB Single Crystal Lineshape and Dynamic Parameters. *physica status solidi (b)* **1987**, *142*, 461−471.
(99) Scholes, G. D. Limits of exciton delocalization in molecular aggregates. *Faraday Discuss.* **2020**, *221*, 265−280.
(100) Giannini, S.; Peng, W.-T.; Cupellini, L.; Padula, D.; Carof, A.; Blumberger, J. Exciton transport in molecular organic semiconductors

https://doi.org/10.1021/acs.jpcc.4c02941
J. Phys. Chem. C XXXX, XXX, XXX−XXX

boosted by transient quantum delocalization. *Nat. Commun.* **2022**, *13*, 2755.
(101) Tait, C. E.; Neuhaus, P.; Peeks, M. D.; Anderson, H. L.; Timmel, C. R. Transient EPR Reveals Triplet State Delocalization in a Series of Cyclic and Linear -Conjugated Porphyrin Oligomers. *J. Am. Chem. Soc.* **2015**, *137*, 8284−8293.
(102) Tait, C. E.; Neuhaus, P.; Anderson, H. L.; Timmel, C. R. Triplet State Delocalization in a Conjugated Porphyrin Dimer Probed by Transient Electron Paramagnetic Resonance Techniques. *J. Am. Chem. Soc.* **2015**, *137*, 6670−6679.
(103) Meyer, D. L.; Matsidik, R.; Sommer, M.; Biskup, T. Electronic Structure Trumps Planarity: Unexpected Narrow Exciton Delocalization in PNDIT2 Revealed by Time-Resolved Electron Paramagnetic Resonance (EPR) Spectroscopy. *Advanced Electronic Materials* **2018**, *4*, 1700385.
(104) Zhang, G.; Chen, X.-K.; Xiao, J.; Chow, P. C. Y.; Ren, M.; Kupgan, G.; Jiao, X.; Chan, C. C. S.; Du, X.; Xia, R.; et al. Delocalization of exciton and electron wavefunction in non-fullerene acceptor molecules enables efficient organic solar cells. *Nat. Commun.* **2020**, *11*, 3943.
(105) Tiago, M. L.; Northrup, J. E.; Louie, S. G. Ab initio calculation of the electronic and optical properties of solid pentacene. *Phys. Rev. B* **2003**, *67*, 115212.
(106) Refaely-Abramson, S.; da Jornada, F. H.; Louie, S. G.; Neaton, J. B. Origins of Singlet Fission in Solid Pentacene from an ab initio Green's Function Approach. *Phys. Rev. Lett.* **2017**, *119*, 267401.
(107) Shushin, A. I. Manifestation of specific features of T-exciton migration in magnetic field effects on TT-annihilation in molecular crystals: Analysis of low-field resonances. *J. Chem. Phys.* **2019**, *151*, 224503.
(108) Shushin, A. I.; Umanskii, S. Y.; Chaikina, J. A. Kinetics of the Decay of Excited Singlet State into a Pair of T-Excitons in Rubrene Films: Mechanism and Manifestation of Exciton Migration. *Russian Journal of Physical Chemistry B* **2023**, *17*, 1403−1408.
(109) Bayliss, S.; Kraffert, F.; Zhang, C.; Bittl, R.; Behrends, J. Tuning Spin Dynamics in Crystalline Tetracene. *J. Phys. Chem. Lett.* **2019**, *10*, 1908−1913.
(110) El-Sayed, M. A. Optical Pumping of the Lowest Triplet State and Multiple Resonance Optical Techniques in Zero Field. *J. Chem. Phys.* **1971**, *54*, 680−691.
(111) Zhu, T.; Wan, Y.; Guo, Z.; Johnson, J.; Huang, L. Two Birds with One Stone: Tailoring Singlet Fission for Both Triplet Yield and Exciton Diffusion Length. *Adv. Mater.* **2016**, *28*, 7539−7547.
(112) Wan, Y.; Wiederrecht, G. P.; Schaller, R. D.; Johnson, J. C.; Huang, L. Transport of Spin-Entangled Triplet Excitons Generated by Singlet Fission. *J. Phys. Chem. Lett.* **2018**, *9*, 6731−6738.
(113) Vong, D.; Maleki, F.; Novak, E. C.; Daemen, L. L.; Moulé, A. J. Measuring Intermolecular Excited State Geometry for Favorable Singlet Fission in Tetracene. *J. Phys. Chem. Lett.* **2024**, *15*, 1188−1194.
(114) Smith, M. B.; Michl, J. Recent Advances in Singlet Fission. *Annu. Rev. Phys. Chem.* **2013**, *64*, 361−386.

https://doi.org/10.1021/acs.jpcc.4c02941
J. Phys. Chem. C XXXX, XXX, XXX−XXX